Central Power Research Institute

Vol. 18(2)/139-147, December 2022
ISSN (Print) : 0973-0338
DOI : 10.33686/pwj.v18i2.1103

Power Research

Fast Charging Behaviour of High-Power Li-Ion Cell at Different Temperatures and Effect on Capacity and Internal Resistance

N. Srilekha, Kuldeep Rana*, Pradeep Kumar, Shashank K. Ravanikar, P. Chandrashekar

Electrical Appliances Technology Division, Central Power Research Institute, PB No 8066, Prof CV Raman Road, Sadashivanagar PO, Bangalore – 560080, Karnataka, India; kuldeeprana@cpri.in

Abstract

Lithium-Ion Batteries (LIBs), which have already proven to be a reliable power source in consumer electronics devices, are being considered a viable option for powering Electric Vehicles (EVs). Fast charging of EVs is one of the key challenges that is preventing a wide range of adoption of EVs. In this study, a lithium-ion cell with Lithium Titanium Oxide (LTO)-lithium Nickel Manganese Cobalt oxide (NMC) chemistry of 30 Ah has been used to study the fast charging capabilities at different temperatures and C-rates. Various parameters such as temperature rise, nominal and exponential capacity, and internal resistance have been studied for different C-rates (C/3, 1C, and 2C) and at different temperatures (25 °C, 40 °C, and -10 °C). The ΔV values along with the charge and discharge characteristics have been analyzed, and the experimental results are compared with the simulation results.

Keywords: Fast Charging, High Energy Density, Internal Resistance, Lithium-Ion Battery, LTO-NMC

1. Introduction

The global concerns of environmental change and the fuel crisis have been the major factors in the adoption of other means of energy production, energy storage, and electrified transportation. In recent years, a huge penetration of different types of Electric Vehicles (EVs) has been observed[1]. An electric vehicle is easy to operate, provides zero emissions, and greatly impacts the fuel cost as compared to conventional vehicles. Electric vehicles are gaining popularity because they run by considering only electricity as the main fuel. These EVs are classified primarily as Hybrid Electric Vehicles (HEVs), Plug-In Electric Vehicles (PHEVs), and pure Battery Electric Vehicles (BEVs)[2]. A vehicle is a combination of different subsystems which interact with each other to make the electric vehicle work efficiently and effectively[3]. An electric vehicle consists of unique constituents like an electric motor, a power converter, a Battery Management System (BMS), and a battery pack[4]. The development of secondary battery systems has played a major role in the development of EVs. There are different choices of Li-ion batteries available which have different energy densities, power density characteristics, voltage ranges, safety and cost. The EV integrated with a battery pack consists of lithium-ion cells and a battery management system to control the battery pack while in use, like when driving, breaking, charging, communicating, and safety.

The battery pack is the building block for the electric vehicle, which acts as the main energy storage source for EV propulsion and other components. The battery pack in an EV is monitored and controlled by a Battery Management System (BMS). The main role of the BMS is to ensure the safety of the vehicle and is responsible for energy management. Among the various battery chemistries available, the selection of a safe, high energy and power density battery with fast charging is important for any particular application. The Lithium-Ion Battery

*Author for correspondence

(LIB), which has high energy density, low self-discharge rate, high voltage, long lifespan, high reliability, and fast recharging characteristics, is the main contender for EVs[5]. These LIBs, which are exposed to severe operating conditions, have been investigated in a previous publication in detail for different applications[7]. The LIB is comprised of five different components, i.e., cathode, anode, electrolyte, separator, and current collectors. The working of these elements begins with choosing the cathode and anode materials. There are different types of Li-ion batteries depending on their cathode and anode chemistry.

Lithium Iron Phosphate (LFP) has a lower cost, high safety, good thermal stability, a longer lifetime, and a low self-discharging rate. However, it has lower specific energy as compared to Lithium Manganese Oxide (LMO), which is another cathode material with low cost, but it offers less capacity and increased capacity losses on storage and cycle life, hence it is less preferable to be used in Evs[8,9]. Lithium Cobalt Oxide (LCO) is being used traditionally in portable electronic devices due to its low cost, less availability in nature, and its toxic nature[8]. Lithium Nickel Cobalt Aluminum oxide (NCA) offers somewhat similar characteristics to NMC and is more suitable for use in EVs for long-range and high power, but the cost and safety need more attention for such cathode chemistry.

The focus of the study is to understand the behaviour of fast-charging chemistry based on Lithium Titanium Oxide (LTO), which can be used as an anode. It offers advantages in terms of high power and an extraordinary life cycle and is much safer as compared to other chemicals. LTO has a spinal structure and is known as a "zero-strain" material as there is no volume change during the charging and discharging of the battery. $Li_4Ti_5O_{12}$ has an eminently long cycle life and calendar life, a high power capability, and incomparable safety features[5,11]. Hence, in this study, an LTO-based commercial cell has been selected, which is combined with an NMC-based cathode to maximize the cell voltage.

NMC-based chemistry has demonstrated a maximum specific energy of 174 Wh/kg, which is one of the largest values compared to other chemistries[13]. LTO has engrossing attributes as it has a high discharge plateau of 1.55 V vs $Li^{+/Li0}$ [14]. Thus, to achieve higher capacity from LTO-based anode materials, it is required to couple with the cathode with a higher potential Vs Li/Li^{+}. Various studies have already been carried out on LTO-based anode materials with different cathode chemistries[15,17].

In this work, a commercial cell of LTO-NMC chemistry has been selected in order to understand the various performance parameters such as discharge capacity, charging capacity, fast charging characteristics, and temperature rise of the cell when electrochemical performance has been carried out at various temperatures and different C-rates[18]. The effects of temperature and C-rate of Li-ion batteries on DCIR have been analyzed[19,20]. The study of DCIR is very important to understand the state of health of the battery at different C-rates and temperatures for EV's. The internal resistance also gives information about power performance, regenerative braking capabilities, dynamic charge and discharge efficiencies, or physical degradation of the battery. The internal resistance varies with different C-rates and temperatures[21,22].

The experimental data for high-power battery discharge profiles at various temperatures and C-rates were compared to the simulated results. The modelling part of the battery simulation in MATLAB/Simulink has been carried out, analyzed and compared with the experimental data[23,24]

2. Experimental Set-up

Table 1. Specifications of li-ion cell (LTO-NMC)

Top Diameter(m)	66.2
Middle Diameter(m)	66.6
Bottom Diameter(m)	66.4
Length (m)	161.2
Weight (kg)	1.183
Ah Rating	30 Ah
Nominal voltage	2.3 V

Table 1 shows the specifications of the high-power commercial LTO-NMC cell used in experiments carried out. Figure 1 shows the experimental setup of a high-power Li-ion cell. The experimental setup is incorporated with the cylindrical LTO-NMC cell, which is connected with cables to measure the voltage, current, power, and energy with respect to time. A thermocouple will be connected to one terminal of the cell which measures the corresponding temperature of the cell during the charge and discharge process.

The other side of the cables is connected to the battery life cycle tester (Bitrode), which performs the charge and discharge cycling of batteries, in which various parameter

functions are incorporated, and is connected to a server which gives its output corresponding to the given input. The battery life cycle tester, i.e., Bitrode, is operated through VisualCN software. In the VisualCN software, the programming has been done by giving corresponding commands and considering rest, charge, and discharge conditions. The LCN bitrode is connected to the host computer. The data can be collected based on the sample time given.

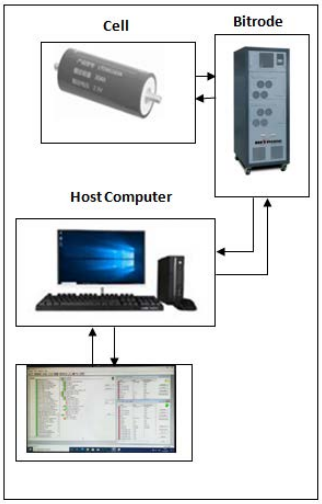

Figure 1. The experimental setup of a high-power Li-ion cell (30 ah, 2.3 v).

Figure 2 shows the block diagram used to validate the experimental results of the high-power Li-ion cell in MATLAB/Simulink. For the verification of the experimental tests with the simulation results, an ideal battery has been chosen and the respective parameters such as max. voltage, rated capacity, discharge characteristics, temperature effects, etc. have been fed to the ideal battery. The results show that the conducted experimental tests and the simulation results have been analysed and matched appropriately.

The results were validated at different temperatures, and all the results were almost matched, which shows that results can also be validated at different SOC.

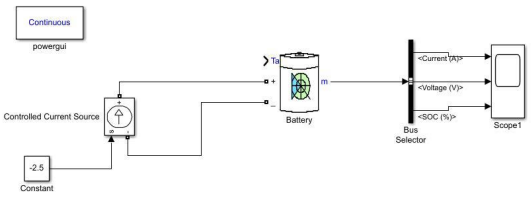

Figure 2. Discharge profile characteristics for high-power lithium-ion cell using matlab Simulink.

3. Charge/Discharge Performance

Charge/discharge profiles are important to understand the battery conditions and battery performance to confirm the rated parameters such as Ah-rating at different C-rates. The discharge profile of the battery gives the storage of energy in terms of a specified end voltage, a specified current, and a specified time. The capacity test majorly includes charging and discharging a battery at different C-rates. The charging of Li-ion batteries is done using constant Current-Constant Voltage (CC-CV). Here the CC method has been carried out, which is more accurate for regenerative braking and fast charging of the EV. The CC method is performed at different temperatures and C rates. The test is started by giving a rest condition, followed by charging the battery by applying constant current until the voltage reaches the upper cut-off voltage. According to battery specifications, the lower and upper cut-off voltages are 1.5 and 2.8 V, respectively. The test is implemented for different C-rates (C/3, 1C, 2C) and at different temperatures (25 °C, 40 °C, and -10 °C). Various parameters at different conditions have been analysed, such as variation in capacity at different C-rates and temperatures, cut-off conditions, nominal voltage, temperature rise, and internal resistance of the cell at various test conditions.

4. Results and Discussion

Figure 3 (A) represents the charge/discharge profile for a high-power lithium-ion cell at room temperature (25 °C) at different C-rates, i.e., C/3,1C and 2C. The voltage during the charging increases from the lower cut-off voltage(1.5 V) to the nominal voltage and then rises smoothly to the upper cut-off voltage of the cell (2.8 V). The charge capacities observed are 36, 35, and 33 Ah at C/3, 1C, and 2C respectively, which have been calculated by multiplying the time taken and constant current used for the charging of the battery. To understand the effect of charging performance at different temperatures, tests have been carried out at -10 and 40 °C and the profiles are demonstrated in Figure 3 (B and C) at different C-rates. The charging capacity values at 40 °C are 35, 34.5, and 34 Ah at C/3, 1C, and 2C respectively. The charge/discharge profile shown in Figure 4 (C) at -10 °C demonstrates charging capacities of 31, 32.1, and 33 Ah at C/3, 1C, and 2C, respectively. From the charge profile, it is observed that for the higher C-rate, the capacity reduces as compared

to the lower C-rate due to the various electrochemical phenomena such as increased internal resistance and slow diffusion of ions[12].

The discharge profiles are shown in Figure 3 (A), (B), and (C) at different temperatures, namely ambient, -10, and 40 ˚C respectively. At room temperature, the capacities are 34.6 Ah, 33.5 Ah, and 33 Ah at C/3, 1C, and 2C, respectively at 40 ºC, the capacities are 35 Ah, 34.2 Ah, and 34 Ah at C/3, 1C, and 2C, respectively at -10 ºC, the capacities are 27.6 Ah, 25.4 Ah, and 25 Ah respectively. Higher C-rates and low temperatures lead to a fading in discharge capacities due to the slowing down of electrochemical reactions and ionic diffusion.

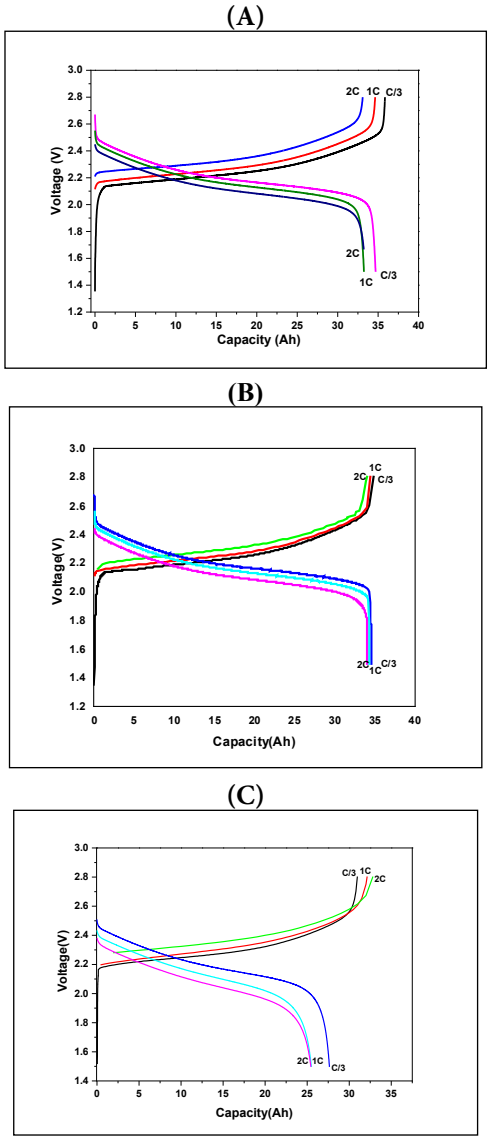

Figure 3. Charge/discharge profile for high-power lithium ion cell (2.3 v 30 ah, nmc-lto) at rt, 40 °C & -10 °C and different c rates (C/3, 1C and 2C).

From the charge and discharge capacities, the efficiency of the cell can be calculated by using the capacity achieved, which is called the coulombic efficiency of the cell, and it is expressed by using the formula[28,29]

$$Columbic\ efficiency(\eta) = \frac{Cdischarge}{Ccharge} * 100 \quad (1)$$

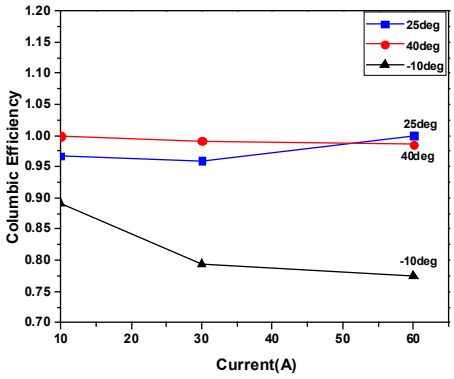

Figure 4. Variation of Columbic efficiency w.r.t different current i.e., C-rates and also at different temperatures.

The Columbic efficiency is less as the C-rate, i.e., the current is higher and the internal resistance is also higher in discharge conditions, hence discharge power will also be reduced. The efficiency achieved at 25°C is 96.7%, 96%, and 99.9 % at C/3, 1C, and 2C respectively. At 40 °C, the efficiency is 99.9%, 99.1%, and 98.5% at C/3, 1C, and 2C, respectively. The efficiency achieved at -10 °C is 89.2%, 79.4% and 77.5 % at C/3, 1C and 2C respectively. The efficiency at 40 and 25°C is higher compared to -10°C, and there is an appropriate reduction in efficiency with respect to the C-rates. Figure 4 shows the Columbic efficiency graph.

Figure 5 represents the variation of the effects of different cell temperatures at different C-rates. The graph is plotted by considering capacity (Ah) on the X-axis and cell temperature (°C) on the Y-axis. From the plot, we can observe the capacity achieved at different cell temperatures varies with different C-rates. And also, the temperature is a changing parameter in the li-ion battery. Figure 5 (A, B, and C) also represent the variation in cell temperature at different ambient temperatures (25 °C, 40 °C, and -10°C).

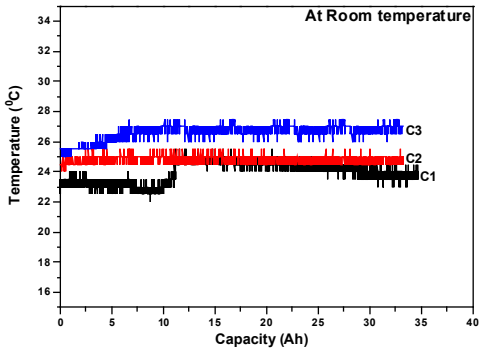

(A)

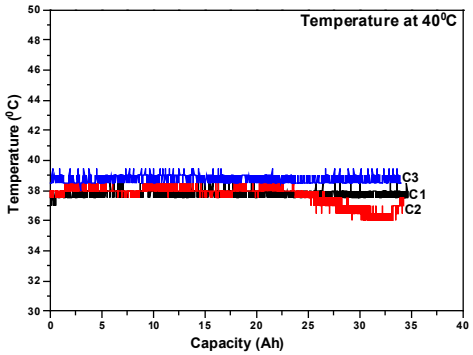

(B)

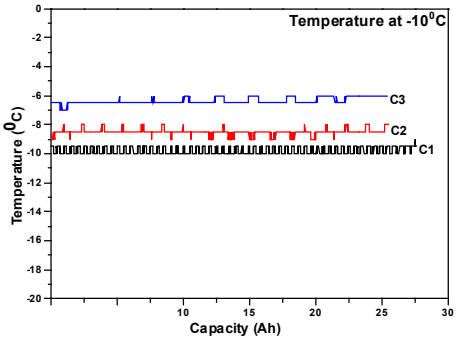

(C)

Figure 5. Variation of temperature (25 °C, 40 °C and -10 °C) with different capacity for high power lithium ion cell (2.3 V 30 Ah, NMC-LTO) and at different (C/3, 1C and 2C) rates.

The temperature is mainly influenced by internal resistance. The internal resistance decreases as the temperature increases because of the ions that acquire more energy and lead to the resistance offered to their movement being reduced considerably. Also, as the C–rate increases, the temperature of the cell measured at one of the metallic terminals increases, which leads to excess heat generation. This is an important parameter to be observed in real driving conditions for the safety of the vehicle and passengers.

Figure 6 (A), (B), and (C) shows the discharge profile characteristics of high-profile Li-ion cells at 25 °C, 40 °C, and -10°C and different C-rates.

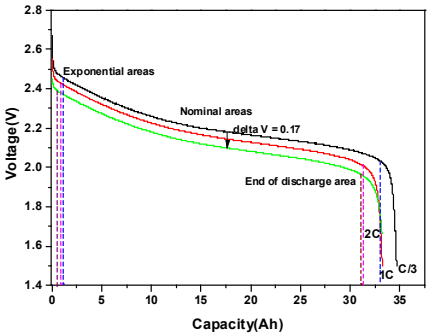

(A)

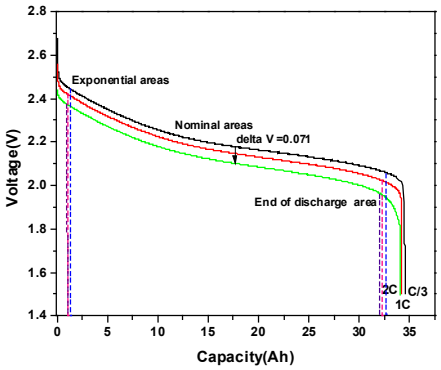

(B)

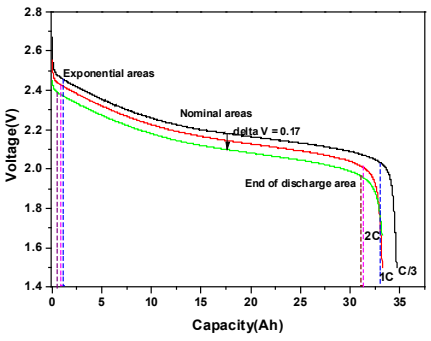

(C)

Figure 6. Discharge profiles of high-power Li-ion cell (30 AH,2.3 V).

Table 2. Discharge profile areas and DCIR at different C-rates and 25 °C temperature

Diff. C rates	Capacities at different areas				
	EC (Ah)	NC (Ah)	EDC (Ah)	Total (Ah)	DCIR (Ω)
C/3	1.6	31.3	1.77	34.7	0.0142
1C	0.8	30.5	1.91	33.2	0.005
2C	0.4	30.8	1.96	33.2	0.002

EC: Exponential Capacity
NC: Nominal Capacity
EDC: End of Discharge Capacity
DCIR: Discharge Internal Resistance

Table 3. Discharge profile areas and DCIR at different C-rates and at 40 °C temperature

Diff. C rates	Capacities at different areas				
	EC (Ah)	NC (Ah)	EDC (Ah)	Total (Ah)	DCIR (Ω)
C/3	1.35	31.2	2.01	34.7	0.0149
1C	1.12	31.15	1.96	34.2	0.005
2C	1.04	31.10	1.89	34	0.002

EC: Exponential Capacity
NC: Nominal Capacity
EDC: End of Discharge Capacity
DCIR: Discharge Internal Resistance

The entire discharge curve can be divided into three distinct regions, starting the voltage drops quickly in the initial stage, where the higher the discharge rate, the more the drop will be. Next, the voltage drop will be less as the cell discharges slowly; here the area of the discharge will be greater.

Finally, the cell starts to drop sharply until it reaches the cut-off voltage (1.5 V). The discharging capacity achievement will be less at lower temperatures, i.e., -10°C and at higher C-rates. It's because the dynamic voltage of the battery drops faster and reaches the cut-off voltage before the ions move out.

Table 4. Discharge profile areas and DCIR at different C-rates and at -10 °C temperature

Diff.C rates	Capacities at different areas				
	EC (Ah)	NC (Ah)	EDC (Ah)	Total (Ah)	DCIR (Ω)
C/3	0.66	23.93	3.05	27.6	0.0057
1C	1.14	21.3	2.99	25.4	0.0034
2C	1.24	20.52	3.67	25	0.00253

EC: Exponential Capacity
NC: Nominal Capacity
EDC: End of Discharge Capacity
DCIR: Discharge Internal Resistance

The different discharging capacities achieved in each area at different C-rates can be observed from different graphs and have been tabulated as shown in Tables 2, 3, and 4 along with discharge internal resistance. The variation in different discharge curves at different C-rates can be evaluated from the parameter ΔV, i.e., defined as the change in nominal voltage area at different C-rates. The ΔV values achieved with respect to different discharge curves are 0.17, 0.071, and 0.13 at 25 °C, 40 °C, and -10°C. And these values are not exactly as they are often adjusted for the better fit of the curve. From the charge/discharge profiles, the Discharge Internal Resistance (DCIR) has also been calculated by using the formula,

$$DCIR = \frac{\Delta V}{\Delta I} \quad (2)$$

Figure 8 represents the simulated discharge profile of a high-power Li-ion cell at 25 °C, 40 °C, and -10 °C and at different C-rates. The simulation results show the 3 distinct discharge regions similar to the experimental discharge curves discussed in Figure 6. Here, a controlled current source has been used to maintain the constant specific current with respect to the source. In addition, simulation results tell us about the area with respect to the different discharge capacity curves. Exponential values in different discharge curves go on decreasing at different temperatures.

Exponential values at 25 °C and -10 °C are exactly matched, and at 40 °C, there is a slight variation of 0.1 % between the simulated and experimental results.

The discharge capacity values achieved at different temperatures were appropriately matched with a variation of ±1-2 % between the simulated and the experimental results.

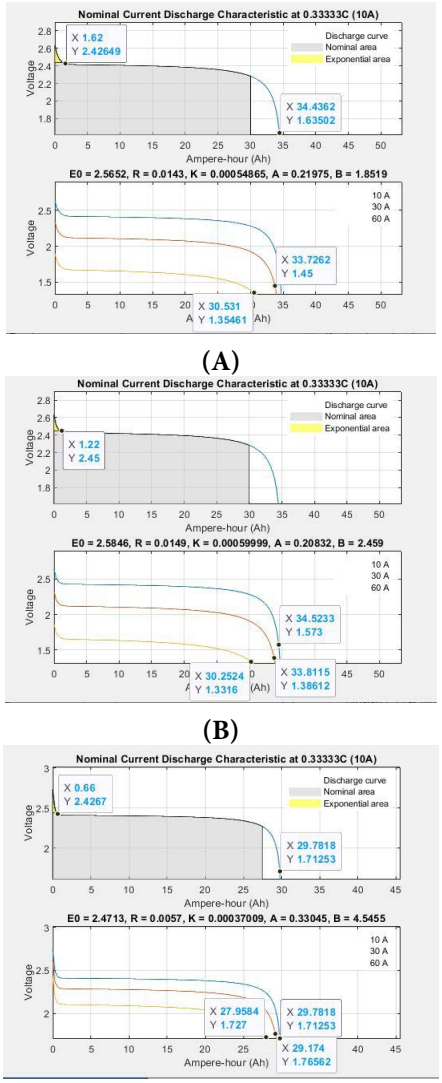

Figure 7. Simulated discharge profiles of high-power Li-ion cells at different C-rates and different temperatures (25 °C, 40 °C and -10 °C)

5. Conclusion

In this work, performance parameters such as internal resistance, ΔV, nominal capacity and exponential capacity have been analysed for different temperatures, C-rates and charging/discharging profiles, and the capacity achieved at 40 °C and 25 °C is higher and goes on reducing at lower temperatures (-10°C). The results show that internal resistance at different temperatures does not vary significantly with the ambient temperature and that the internal resistance affects the voltage, current, and power supplied to the load. The ΔV value shows much variation at lower temperatures for different C-rates. The capacity reduces at the lower temperature because of the increase in the resistance of the electrolyte and the rate of transfer of energy significantly decreases. The charging has been carried out at a high C-rate (2C), which enables fast charging of batteries.

The experimental and simulation results were analyzed and they are appropriately matched with a slight variation of ±1-2 %.

Overall, the high energy density, high power density, and longer life cycle characteristics of Li-ion batteries make them more suitable for EV adoption.

6. Acknowledgement

The authors would like to thank the management of Central Power Research Institute, an autonomous institute under the Ministry of Power for their support in conducting the following research work - "Fast Charging behaviour of high power Li-ion cell at different temperatures and effect on capacity and internal resistance".

7. References

1. Zhang YC, Briat O, Deletage J-Y, *et al.* Performance quantification of latest generation Li-ion batteries in wide temperature range. IECON 2017 - 43rd Annual Conference of the IEEE Industrial Electronics Society; 2017. p. 7666-7671. https://doi.org/10.1109/IECON.2017.8217343
2. Andwari AM, Pesiridis A, Rajoo S, *et al.* A review of Battery Electric Vehicle technology and readiness levels. Renewable and Sustainable Energy Reviews. 2017; 78. https://doi.org/10.1016/j.rser.2017.03.138
3. Un-Noor F, Padmanaban S, *et al.* A comprehensive study of key Electric Vehicle (EV) components, technologies, challenges, impacts, and future direction of development. Energies. 2017; 10(8):1217. https://doi.org/10.3390/en10081217
4. Hannan MA, Hoque MM, Hussain, *et al.* State-of-the-art and energy management system of lithium-ion batteries in electric vehicle applications: Issues and recommendations. IEEE Access. 2018; 6:19362-19378. https://doi.org/10.1109/ACCESS.2018.2817655
5. Yu M, Hynan P, *et al.* Current Li-ion battery technologies in electric vehicles and opportunities for advancements. Energies. 2017; 12(6):1074. https://doi.org/10.3390/en12061074
6. Katari JS, Sneha R, Vinayaka KU, *et al.* A concise review of different standards for performance testing of lithi-

um-ion batteries for electric vehicle applications. IEEE International Conference on Power Systems Technology (POWERCON); 2020. p. 1-6. https://doi.org/10.1109/POWERCON48463.2020.9230560

7. Bank T, Feldmann J, Klamor S, *et al*. Extensive aging analysis of high-power lithium titanate oxide batteries: Impact of the passive electrode effect. Journal of Power Sources. 2020; 473: 228566. ISSN0378-7753. https://doi.org/10.1016/j.jpowsour.2020.228566
8. Stan A, Swierczyński M, Stroe D, *et al*. Lithium ion battery chemistries from renewable energy storage to automotive and back-up power applications - An overview. International Conference on Optimization of Electrical and Electronic Equipment (OPTIM); 2014. p. 713-720. https://doi.org/10.1109/OPTIM.2014.6850936
9. Foad HG, Jaguemont J, Goutam S, *et al*. Concept of reliability and safety assessment of lithium-ion batteries in electric vehicles: Basics, progress, and challenges. Applied Energy. 2019; 251:113343. ISSN 0306-2619. https://doi.org/10.1016/j.apenergy.2019.113343
10. Chen Z, Belharouak I, Sun, *et al*. Titanium-based anode materials for safe lithium-ion batteries. Adv Funct Mater. 2013; 23:959-969. https://doi.org/10.1002/adfm.201200698
11. Rana K, Kim SD, Ahn JH. Additive-free thick graphene film as an anode material for flexible lithium-ion batteries. Nanoscale. 2015; 7(16):7065-7071. https://doi.org/10.1039/C6TA09059A
12. Wang Y, Chu Z, Feng X, *et al*. Overcharge durability of Li4Ti5O12 based lithium-ion batteries at low temperature. Journal of Energy Storage. 2018; 19:302-310. ISSN-2352-152X. https://doi.org/10.1016/j.est.2018.08.012
13. Nikolian A, Jaguemont J, de Hoog J, *et al*. Complete cell-level lithium-ion electrical ECM model for different chemistries (NMC, LFP, LTO) and temperatures (−5 °C to 45 °C) - Optimized modelling techniques. International Journal of Electrical Power and Energy Systems. 2018; 98:133-146. ISSN-0142-0615. https://doi.org/10.1016/j.ijepes.2017.11.031
14. Gauthier N, Courreges C, Demeaux J, *et al*. Probing the in-depth distribution of organic/inorganic molecular species within the SEI of LTO/NMC and LTO/LMO batteries: A complementary ToF-SIMS and XPS study. Applied Surface Science. 2020; 501:144266. ISSN-0169-4332. https://doi.org/10.1016/j.apsusc.2019.144266. https://doi.org/10.1016/j.apsusc.2019.144266
15. Barai A, Uddin K, Dubarry M, *et al*. A comparison of methodologies for the non-invasive characterisation of commercial Li-ion cells. Progress in Energy and Combustion Science. 2019; 72:1-31. ISSN 0360-1285. https://doi.org/10.1016/j.pecs.2019.01.001
16. Gao Y, Zhang X, Cheng QB, *et al*. Classification and review of the charging strategies for commercial lithium-ion batteries. IEEE Access, 2019; 7:43511-43524. https://doi.org/10.1109/ACCESS.2019.2906117
17. Zeng X, Li M, Abd, *et al*. Commercialization of Lithium Battery Technologies for Electric Vehicles. Adv Energy Mater. 2019, 9:1900161. https://doi.org/10.1002/aenm.201900161
18. Abdel-Monem M, Trad K, Omar N, *et al*. Influence analysis of static and dynamic fast-charging current profiles on ageing performance of commercial lithium-ion batteries. Energy. 2017; 120:179-191. ISSN 0360-5442. https://doi.org/10.1016/j.energy.2016.12.110
19. Liu Z, Gao Y, Chen H, *et al*. Thermal performance of lithium titanate oxide anode based battery module under high discharge rates. World Electric Vehicle Journal. 2021; 12(3):158. https://doi.org/10.3390/wevj12030158
20. Cicconi P, Landi D, Germani M, Thermal analysis and simulation of a Li-ion battery pack for a lightweight commercial EV. Applied Energy. 2017; 192:159-177. ISSN 0306-2619. https://doi.org/10.1016/j.apenergy.2017.02.008
21. Ansean D, Gonzalez M, Viera JC, *et al*. Electric vehicle li-ion battery evaluation based on internal resistance analysis. IEEE Vehicle Power and Propulsion Conference (VPPC); 2014. p. 1-6. https://doi.org/10.1109/VPPC.2014.7007058
22. Belt JR, Ho CD, Motloch CG, *et al*. A capacity and power fade study of Li-ion cells during life cycle testing. Journal of Power Sources. 2003; 123(2):241-246. ISSN 0378-7753, https://doi.org/10.1016/S0378-7753(03)00537-8
23. Cittanti D, Ferraris A, Airale A, *et al*. Modeling Li-ion batteries for automotive application: A trade-off between accuracy and complexity. International Conference of Electrical and Electronic Technologies for Automotive; 2017. p. 1-8. https://doi.org/10.23919/EETA.2017.7993213
24. Nemes R, Ciornei S, Ruba M, Hedesiu, H, et al. Modeling and simulation of first-order Li-Ion battery cell with experimental validation. 8th International Conference on Modern Power Systems (MPS); 2019. p. 1-6. https://doi.org/10.1109/MPS.2019.8759769
25. Naha A, Han S, Agarwal S. *et al*. An incremental voltage difference based technique for online state of health estimation of Li-ion batteries. Sci Rep. 2020; 10:9526. https://doi.org/10.1038/s41598-020-66424-9 PMid:32533023 PMCid:PMC7293255
26. Samadani E, Farhad S, Panchal, *et al*. Modeling and evaluation of li-ion battery performance based on the electric vehicle field tests. SAE Technical Papers; 2014. https://doi.org/10.4271/2014-01-1848
27. Mushini JCD, Rana K, Aspalli MS. Analysis of open circuit voltage and state of charge of high power lithium ion battery. International Journal of Power Electronics and Drive

Systems (IJPEDS). 2022 Jun; 13(2):657-664. ISSN:2088-8694. https://doi.org/10.11591/ijpeds.v13.i2.pp657-664

28. Tornheim A, O'Hanlon DC. What do coulombic efficiency and capacity retention truly measure? a deep dive into cyclable lithium inventory, limitation type, and redox side reactions. J Electrochem Soc. 2020; 167:110520 https://doi.org/10.1149/1945-7111/ab9ee8
29. Liu Y, Zhang L, Jiang J, *et al*. A data-driven learning-based continuous-time estimation and simulation method for energy efficiency and coulombic efficiency of lithium ion batteries. Energies. 2017; 10:597. https://doi.org/10.3390/en10050597
30. Yang F, Zhao Y, Tsui K-L, Bae, *et al*. A study of the relationship between coulombic efficiency and capacity degradation of commercial lithium-ion batteries. Energy. 2018; 145. https://doi.org/10.1016/j.energy.2017.12.144
31. Feng F, Lu, R, Zhu, *et al*. A combined state of charge estimation method for lithium-ion batteries used in a wide ambient temperature range. Energies. 2014; 7:3004-3032. https://doi.org/10.3390/en7053004
32. Qiu C, He G, Shi W, *et al*. The polarization characteristics of lithium-ion batteries under cyclic charge and discharge. J Solid State Electrochem. 2019; 23:1887-1902. https://doi.org/10.1007/s10008-019-04282-w
33. Liu Z, Wang C, Guo X, *et al*. Thermal characteristics of ultrahigh power density lithium-ion battery. Journal of Power Sources. 2021; 506:230205. ISSN-0378-7753, https://doi.org/10.1016/j.jpowsour.2021.230205